Computing Method Applied for Simulation and Forecast of Hydrophysical Fields in the Southeastern Black Sea

DEMURI DEMETRASHVILI
M. Nodia Institute of Geophysics,
I. Javakhishvili Tbilisi State University,
M. Aleksidze str., 1, Tbilisi,
GEORGIA

also with
Institute of Hydrometeorology,
Georgian Technical University,
David Agmashenebeli str., 150, Tbilisi,
GEORGIA

Abstract: - In this paper, a numerical regional model of the Black Sea hydrodynamics with a spatial resolution of 1 km is applied to simulate and forecast the mesoscale circulation and thermohaline structure in the southeastern part of the Black Sea. The regional model is based on a nonlinear nonstationary system of differential equations in z coordinates, describing the evolution of three-dimensional fields of currents, temperature, salinity, and density. The solution of the equation system is based on the use of finite-difference methods, in particular, on the method of multicomponent splitting of the differential operator of the original problem into simpler operators. To illustrate the implementation of the numerical model, the paper presents the calculated fields of flow, temperature, and salinity for the summer season of 2020 under real atmospheric forcing derived from the atmospheric model SCIRON. The influence of basin-scale processes on regional processes was taken into account by boundary conditions on the liquid boundary separating the regional area from the open part of the sea basin. A comparison of the forecast results with available satellite data shows that the model reproduces well the basic peculiarities of hydrophysical fields.

Key-Words: - Black Sea, circulation, system of equations, boundary conditions, splitting method, atmospheric forcing, mesoscale eddies.

Received: May 13, 2024. Revised: September 25, 2024. Accepted: October 27, 2024. Published: November 26, 2024.

1 Introduction

In recent decades, mathematical modeling methods have become one of the main research tools in physical oceanography. The Study of the hydrothermodynamics of the Black Sea using mathematical models began in the 1970s of the last century. A review and analysis of numerical models of this period are given in monographs, [1], [2]. Numerical models are based on systems of differential equations describing the hydrophysical processes, whose solution is carried out by finite-difference (numerical) methods. In early studies, two types of models were clearly distinguished: diagnostic and prognostic. In diagnostic models, the density field was determined based on observational data (and not during the solution process). This makes it possible to simplify the system of equations, as it eliminates the need to consider the heat and salinity transfer equations, [3]. Prognostic models based on a complete system of ocean hydro- and thermodynamic equations provide a more adequate reproduction of the processes of sea dynamics, [3], [4], [5]. The complete system includes the equations of motion projected on horizontal coordinate axes, the equation of hydrostatics, the continuity equation for an incompressible fluid, heat and salt advection-diffusion equations, and the empirical equation of state of seawater. The pioneering work in this direction was [4], where a prognostic model was developed for simulating basin-scale wind and thermohaline circulation in the Black Sea. To solve the problem, a numerical scheme was used based on the two-cycle method of splitting the problem both into physical processes and spatial variables. This method, which has found wide application in problems of geophysical fluid dynamics and

ecology, significantly simplifies the solution of complex spatial problems and reduces them to the solution of one-dimensional and two-dimensional problems, [6].

Calculations based on diagnostic and prognostic models have made a significant contribution to the study of the dynamic processes of the Black Sea. Analysis of numerical experiments showed that the calculated fields well reflect the basic peculiarities of the hydrological regime, identified from observational data: the main cyclonic circulation, including two internal cyclonic circulations in the western and eastern parts of the sea, the rise of waters in the central parts of the cyclonic circulations, maximum salinity and density in the central part of the cyclonic circulations, which testifies to the upwelling of salty deep waters in the central areas of the cyclonic circulations. In [4] the significant role of the bottom relief in the northern and western parts of the sea basin was shown.

In early studies, the low level of computing resources did not allow the creation of models with high spatial resolution. In [4], the spatial resolution was 37 km, and in most calculations using diagnostic and prognostic models, the spatial resolution was 40-50 km, which was insufficient for a full study of the features of hydrodynamic processes in the Black Sea, especially in coastal/shelf areas, where eddy structures of various sizes are often formed, [7].

The rapid progress of computing technology over the past 30 years has given great impetus to the creation of high-resolution numerical models, which has made the modeling results more reliable and adequate. Currently, a number of publications are devoted to high-resolution modeling of the Black Sea hydrothermodynamics, [8], [9], [10], [11], [12], [13], [14], [15]. Almost all modern models are based on solving systems of non-stationary, non-linear differential equations using finite-difference methods. It should be noted that in most publications the main attention is paid to the study of the upper layer of the sea, which plays an active role in the interaction of the sea and the atmosphere.

The Black Sea hydrodynamic models have found wide application in problems of modeling the spread of oil pollution accidentally entering the sea, [16], [17].

Modern numerical models of sea dynamics have become not only a powerful research tool, but also have created a solid basis for the development of marine short-term forecasting systems for some European seas, similar to weather forecasting systems. Improvements in remote sensing (satellite) methods and assimilation of in situ observation data have also contributed to the development of marine forecasting systems.

A great achievement of the Black Sea operational oceanography is the development of the basin-scale nowcasting/forecasting system at the beginning of the XXI century, [18], [19]. One of the components of the system became the Black Sea regional forecasting system for the southeastern part of the Black Sea, [20]. The regional system is based on the regional model of the Black Sea dynamics (RM-IG) with a spatial resolution of 1 km, which is developed by adapting the basin-scale numerical model with a spatial resolution of 5 km [12] to the southeastern part of the sea basin. In turn, this basin-scale model is an advanced version of [4]. Within the framework of the EU projects, the computational grid of the RM-IG with a spatial resolution of 1 km was nested in the computational grid of the basin-scale model of the Marine Hydrophysical Institute (Sevastopol, Ukraine) with a resolution of 5 km, which ensured the consideration of the impact of hydrothermodynamic processes of the open part on regional processes through the conditional liquid boundary (one-way nesting method).

This paper presents a regional model of sea hydrodynamics and the main aspects of the numerical algorithm for solving the model equation system based on the splitting method. The results of computer implementation of the RM-IG are also discussed.

2 Problem Formulation

To describe nonstationary hydrophysical processes in the Baroclinic Sea, we consider the following system of differential equations (the x coordinate is directed to the east, y to the north, and z is vertically downwards)

$$\frac{\partial u}{\partial t} + div\vec{u}u - lv + \frac{1}{\rho_0}\frac{\partial p'}{\partial x} = D_u^{xy} + D_u^z \qquad (1)$$

$$\frac{\partial \mathrm{v}}{\partial t} + div\vec{u}\mathrm{v} + lu + \frac{1}{\rho_0}\frac{\partial p'}{\partial y} = \mathrm{D}_{\mathrm{v}}^{\mathrm{xy}} + D_v^z, \qquad (2)$$

$$\frac{\partial p'}{\partial z} = g\rho', \qquad div\,\vec{u} = 0, \qquad (3)$$

$$\frac{\partial T'}{\partial t} + div\,\vec{u}T' + \gamma_T.w = \frac{\partial \nu_{\mathrm{T}}\gamma_T}{\partial z} - \frac{1}{c\rho_0}\frac{\partial I}{\partial z} + \qquad (4)$$

$$+ D_T^{xy} + D_T^z,$$

$$\frac{\partial S'}{\partial t} + div\,\vec{u}S' + \gamma_{\mathrm{S}}w = \frac{\partial \nu_{\mathrm{S}}\gamma_{\mathrm{S}}}{\partial z} + D_S^{xy} + D_S^z, \qquad (5)$$

$$\rho' = \alpha_T T' + \alpha_S S', \quad (6)$$

$$D^{xy}_{u,v} = \frac{\partial}{\partial x}\mu\frac{\partial \Phi}{\partial x} + \frac{\partial}{\partial y}\mu\frac{\partial \Phi}{\partial y} \quad D^{z}_{u,v} = \frac{\partial}{\partial z}\nu\frac{\partial \Phi}{\partial z},$$

$$D^{xy}_{T,S} = \frac{\partial}{\partial x}\mu_1\frac{\partial \Phi}{\partial x} + \frac{\partial}{\partial y}\mu_1\frac{\partial \Phi}{\partial y}, \; D^{z}_{T,S} = \frac{\partial}{\partial z}\nu_1\frac{\partial \Phi}{\partial z},$$

where

$$\Phi = \{u, v, T', S'\},$$

$$\gamma_T = \partial\overline{T}/\partial z, \qquad \gamma_S = \partial\overline{S}/\partial z,$$

$$T = \overline{T}(z) + T', \quad S = \overline{S}(z) + S',$$

$$\rho = \overline{\rho}(z) + \rho', \quad p = \overline{p}(z) + p'$$

$$I = \eta(1-A)I_0\, e^{-\alpha z},$$

$$\alpha_T = \partial f/\partial\overline{T}, \quad \alpha_S = \partial f/\partial\overline{S}.$$

Here *u,* v and *w* represent the components of the flow velocity; *T'*, *S'*, *P'* and ρ' are the deviations of the physical quantities temperature, salinity, pressure, and density from their vertically averaged values $\overline{T}, \overline{S}, \overline{P}$ and $\overline{\rho}$; $l = l_0 + \beta y$ is the Coriolis parameter; I_0 is the total flux of solar radiation to the sea surface determined by the Albrecht formula

[21], A is the albedo of the sea surface; α is the absorption coefficient of solar radiation by seawater; (6) is a linearized formula for the equation of state of seawater ρ = *f* (*T*, *S*) applied in [12]; η is the parameter describing the influence of cloudiness.

μ and ν are the factors of horizontal and vertical eddy viscosities, and μ1 and ν1- are the factors of horizontal and vertical diffusion for heat and salt. Other designations are well known.

The equations (1) - (6) are solved under the following boundary and initial conditions:
On the sea surface z = 0, which is considered a rigid surface, boundary conditions describing atmospheric forcing are:

$$\frac{\partial u}{\partial z} = -\frac{\tau_{z\,x}}{\rho_0\nu}, \quad \frac{\partial v}{\partial z} = -\frac{\tau_{z\,y}}{\rho_0\nu}, \; w = 0,$$

$$\nu_T\frac{\partial T}{\partial z} = Q^T, \qquad \nu_S\frac{\partial S}{\partial z} = (PR - EV)S_0,$$

On the sea bottom z = *H (x, y)*
u = v = w = 0, $\partial T'/\partial z = -\gamma_T$, $\partial S'/\partial z = -\gamma_S$

On the lateral solid surfaces Γ_0
$u = 0,\; v = 0,\; \partial T'/\partial n = 0,\; \partial S'/\partial n = 0.$

On the lateral liquid surfaces Γ_1 two kinds of boundary conditions are considered:
a) in the case of inflow into the sea
$u = \tilde{u}$, $v = \tilde{v}$, $T' = \tilde{T}'$, $S' = \tilde{S}'$,
b) in the case of outflow from the sea
$\partial u/\partial n = 0,\; \partial v/\partial n = 0, \partial T'/\partial n = 0, \partial S'/\partial n = 0,$

Here n is the vector of outer normal to the lateral surface, τ_{zx}, τ_{zy} are wind stress components along the axes x and y; $Q_T = Q'_T/c\rho$, where Q'_T is the turbulent heat flux between the sea and atmosphere;
$\tilde{u}$, $\tilde{v}$, $\tilde{T}'$, $\tilde{S}'$ are the current velocity components along the axes x and y and the deviations of temperature and salinity at the liquid boundary, respectively; *PR* and *EV* are the atmospheric precipitation and evaporation.
$u = u^0$, $v = v^0$, $T' = T'^0$, $S' = S'^0$ at t = 0.

The theorem of uniqueness for the solution of this problem has been proven [2].

The formulas for calculating the factors of horizontal and vertical turbulent viscosity and diffusion were the same as in [20].

The influence of basin-scale processes on regional processes was taken into account by boundary conditions on the liquid boundary separating the regional area from the open part of the sea basin. Values of $\tilde{u}$, $\tilde{v}$, $\tilde{T}'$, $\tilde{S}'$ on the liquid boundary were derived from the basin-scale model of the Black Sea dynamics of the Marine Hydrophysical Institute.

3 Numerical Scheme

For the numerical implementation of the above problem, the two-cycle splitting method was used to split the model equation system both by physical processes and by vertical coordinate planes and lines. Note that in the case of non-commutative operators, the two-cycle splitting method provides second-order accuracy with respect to time, [6].

We will consider the basic stages of the algorithm for solving the system of equations (1) – (6). Before splitting with respect to physical processes, Let's divide the entire time interval (0, T) into equal intervals $t_{j-1} \le t \le t_{j+1}$ (the time step τ = t_{j-1}- t_j) and linearize the equations (1), (2), (4), (5) on each such interval. On each extended interval $t_{j-1} \le t \le t_{j+1}$ we apply the two-cycle method of splitting with respect to physical processes. (for

simplicity, we will omit the primes on the functions *T*, *S*, and *P*).

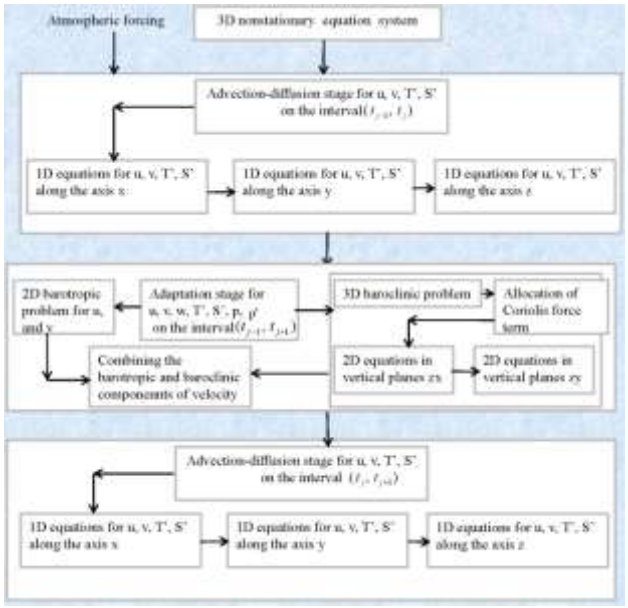

Fig. 1: Block diagram of the numerical algorithm

In order to better understand the numerical solution algorithm, it is shown in Figure 1 in a schematic form.

From Figure 1 it is evident that as a result of splitting the main differential operator of the 3D problem into elementary operators the following basic stages are identified: 1. advection-diffusion stage of physical fields; 2. adaptation of physical fields. At the advection-diffusion stage, the problem is reduced to solving one-dimensional problems, and at the adaptation stage we get two problems: barotropic and baroclinic. As a splitting of baroclinic problem with respect to vertical coordinate planes, it is reduced to a set of two-dimensional problems.

On the time interval, $t_{j-1} \le t \le t_j$ we consider the advection-diffusion stage of physical fields.

$$\begin{aligned}
&\frac{\partial u_1}{\partial t} + div\vec{u}^{\,j} u_1 = D_u^{xy} + D_u^z, \\
&\frac{\partial v_1}{\partial t} + div\vec{u}^{\,j} v_1 = D_v^{xy} + D_v^z, \\
&\frac{\partial T_1}{\partial t} + div\,\vec{u}^{\,j} T_1 = D_T^{xy} + D_T^z + \frac{\partial \nu_T \gamma_T}{\partial z} - \frac{1}{c\rho_0}\frac{\partial I}{\partial z}, \\
&\frac{\partial S_1}{\partial t} + div\,\vec{u}^{\,j} S_1 = D_S^{xy} + D_S^z + \frac{\partial \nu_S \gamma_S}{\partial z},
\end{aligned} \tag{7}$$

where components u^j, v^j, w^j of the vector $\vec{u}^{\,j}$ satisfy the continuity equation:

$$div\vec{u}^{\,j} = 0.$$

System of equations (7) is solved under the above-mentioned boundary conditions and initial data

$u_1^{j-1} = u^{j-1}$, $v_1^{j-1} = v^{j-1}$, $T_1^{j-1} = T^{j-1}$, $S_1^{j-1} = S^{j-1}$. In the second interval $t_{j-1} \le t \le t_{j+1}$ we have the adaptation stage:

$$\begin{aligned}
&\frac{\partial u_2}{\partial t} - lv_2 + \frac{1}{\rho_0}\frac{\partial p_2}{\partial x} = 0, \\
&\frac{\partial v_2}{\partial t} + lu_2 + \frac{1}{\rho_0}\frac{\partial p_2}{\partial y} = 0, \\
&\frac{\partial P_2}{\partial t} = g(\alpha_T T_2 + \alpha_S S_2), \\
&\frac{\partial u_2}{\partial x} + \frac{\partial v_2}{\partial y} + \frac{\partial w_2}{\partial z} = o, \\
&\frac{\partial T_2}{\partial t} + \gamma_T w_2 = 0, \\
&\frac{\partial S_2}{\partial t} + \gamma_S w_2 = 0,
\end{aligned} \tag{8}$$

under boundary conditions:

$w_2 = 0$ at $z = 0, H$

$(\vec{u}_2)_n = 0$

and initial data:

$u_2^{j-1} = u_1^{\,j}$, $v_2^{j-1} = v_1^{\,j}$, $T_2^{j-1} = T_1^{\,j}$, $S_2^{j-1} = S_1^{\,j}$.

Using the equation of state, density is excluded from the hydrostatic equation.

At the last step of splitting, we again have the advection-diffusion stage $(t_j \le t \le t_{j+1})$

$$\begin{aligned}
&\frac{\partial u_3}{\partial t} + div\vec{u}^{\,j} u_3 = D_u^{xy} + D_u^z, \\
&\frac{\partial v_3}{\partial t} + div\vec{u}^{\,j} v_3 = D_v^{xy} + D_v^z, \\
&\frac{\partial T_3}{\partial t} + div\,\vec{u}^{\,j} T_3 = D_T^{xy} + D_T^z + \frac{\partial \nu_T \gamma_T}{\partial z} - \frac{1}{c\rho_0}\frac{\partial I}{\partial z}, \\
&\frac{\partial S_3}{\partial t} + div\,\vec{u}^{\,j} S_3 = D_S^{xy} + D_S^z + \frac{\partial \nu_S \gamma_S}{\partial z},
\end{aligned} \tag{9}$$

System of equations (9) is solved under the same boundary conditions as (7) and initial data:

$u_3^j = u_2^{\,j+1}$, $v_3^j = v_2^{\,j+1}$, $T_3^j = T_2^{\,j+1}$, $S_3^j = S_2^{\,j+1}$.

To approximate in time all nonstationary relatively simple problems received after splitting

the main task, the Crank-Nicholson scheme is used providing second-order accuracy in time.

Note that equations for u, v, *T*, *S* in (7) and (9) on the advection-diffusion stage are independent of each other. Using the two-cycle splitting method with respect to geometrical coordinates x, y, z, and after finite-difference approximation of equations, we obtain a set of one-dimensional problems which are solved effectively by the factorization method.

At the adaptation stage, the solution is divided into barotropic and baroclinic components, i. e. we obtain two problems on the extended time interval $t_{j-1} \le t \le t_{j+1}$. For this purpose we will consider the average on-depth values:

$$\bar{u} = \frac{1}{H}\int_0^H u dz, \quad \bar{v} = \frac{1}{H}\int_0^H v dz \quad \bar{p} = \frac{1}{H}\int_0^H p dz$$

We assume that:

$$u_2 = \bar{u} + u', \; v_2 = \bar{v} + v', \; p_2 = \bar{p} + p', \; T_2 = T', \; S_2 = S'.$$

Then, from (8) we will receive the following equation system for the barotropic problem:

$$\begin{aligned} &\frac{\partial \bar{u}H}{\partial t} - l\bar{v}H + \frac{1}{\rho_0}\frac{\partial \bar{p}H}{\partial x} = 0, \\ &\frac{\partial \bar{v}H}{\partial t} + l\bar{u}H + \frac{1}{\rho_0}\frac{\partial \bar{p}H}{\partial y} = 0, \\ &\frac{\partial \bar{u}H}{\partial x} + \frac{\partial \bar{v}H}{\partial y} = 0. \end{aligned} \tag{10}$$

with boundary condition on the lateral surface σ

$$(\vec{u})_n = 0 \tag{11}$$

The barotropic problem (10)-(11) is reduced to solving a finite-difference system of algebraic equations for integral stream function, which is solved by iterative method.

The operator of the baroclinic problem is preliminary splitting with separating the term of the Coriolis force as an independent stage. Thus, the system of equations is considered:

$$\begin{aligned} &\frac{\partial u}{\partial t} - lv = 0, \\ &\frac{\partial v}{\partial t} + lu = 0. \end{aligned} \tag{12}$$

The analytical solution of (12) is:

$u = u_0 \cos lt + v_0 \sin lt, \; v = v_0 \cos lt - u_0 \sin lt,$

where initial conditions u_0 and v_0 are baroclinic parts of the solution received after the adcection-diffusion stage (9).

The remaining part of the differential operator of the baroclinic problem (without the Coriolis terms) splits into vertical coordinate planes zx and zy. As a result, the adaptation problem is reduced to solving a sequence of similar two-dimensional problems for analogs of the stream function, which are solved using an iterative algorithm.

During the elaboration of the numerical algorithm and corresponding software on “Fortran” the accuracy of the numerical solution of each sub-problem, received as a result of splitting the 3D equation system, was tested as follows: let’s in the area D with lateral surface σ the problem is considered, which in operator form can be written:

$$\frac{\partial \varphi}{\partial t} + A\varphi = f \tag{13}$$

with boundary condition on σ:

$$B\varphi = g \tag{14}$$

and initial condition:

$$\varphi = \varphi^0 \quad \text{at} = 0 \tag{15}$$

where, in general, A and B differential operators, g is given function. Let's choose any analytical function $\bar{\varphi}$, that satisfies the conditions (14), (15) and substitute it into the equation (13). Then we get

$$\frac{\partial \bar{\varphi}}{\partial t} + A\bar{\varphi} = f + \bar{f} \tag{16}$$

The function $\bar{f}$ is defined from equation (16).

It is easy to guess that the numerical solution of the equation:

$$\frac{\partial \varphi}{\partial t} + A\varphi = f + \bar{f}$$

should coincide with the analytical solution $\bar{\varphi}$ with a certain accuracy. In the conducted numerical experiments the accuracy of the numerical solution was evaluated using the formula:

$$\varepsilon = \max\left|\varphi_{k,l} - \bar{\varphi}_{k,l}\right|$$

where *k, l* are the numbers of grid nodes along horizontal axes. Test numerical experiments showed that the value of ε is in the range of 0.002 – 0.007.

4 Model Implementation

The model described above is implemented in the southeastern part of the Black Sea with dimensions of approximately 215x340 km. The maximum sea depth in the model is assumed to be 2006 m. The considered water area covers the Georgian sector of the Black Sea and adjacent area which is allocated from the open sea by meridian 39.08^0E. The southeastern part of the basin is covered with a grid of 215x347 having a horizontal resolution of 1 km. Vertically, 30 calculated horizons were used with a minimum grid step of 2 m near the sea surface and a maximum of 100 m below a depth of 200 m. The time step was 30 minutes. The other parameters had the following values: g = 980 cm/s^2, ρ_0 = 1g/cm^3, l_0 = $0.95.10^{-4}$sec^{-1}, $\beta = 10^{-13}$cm^{-1}sec^{-1}, c = 4.09Jg^{-1}K^{-1} , α = 0.0023m^{-1}, As boundary conditions at the open boundary of the region, we used the fields of currents, temperature and salinity, calculated using the model of the Marine Hydrophysical Institute for the entire sea with a step of 5 km.

Eddy viscosity factor on a vertical:

$$\nu = \begin{cases} 50cm^2/s, & z \le 55m \\ 10cm^2/s, & z > 55m \end{cases}$$

The calculations took into account the inflow of 6 Georgian rivers. atmospheric forcing was derived from the atmospheric model SCIRON.

Calculations based on the RM-IG under real nonstationary atmospheric wind and thermohaline forcing show that the considered water area is characterized by significant seasonal and interannual variability of circulation processes. In the cold season, cyclonic character predominates in the regional circulation, although not infrequently anticyclonic gyre structures can also be observed against the general cyclonic background. In many cases, the summer circulation is distinguished by its anticyclonic character, including the formation of the well-known Batumi eddy in the southeastern part of the sea.

It should be noted that as the calculations carried out under the conditions of real atmospheric forcing show, the Batumi anticyclonic eddy is characterized by different intensities in different years. For example, the Batumi eddy was a very stable formation in 2010, occupying an area approximately 150-200 km in diameter throughout the summer. The circulation regime essentially determines the structure of the salinity field, to which many marine organisms are highly sensitive.

For demonstration purposes, Figure 2 shows the surface current, salinity on z=50 m horizon and the sea surface temperature (SST) corresponding to August 12, 2020 calculated using the RM-IG. The forecasting period was 9-13 August 2020, 00:00 GMT.

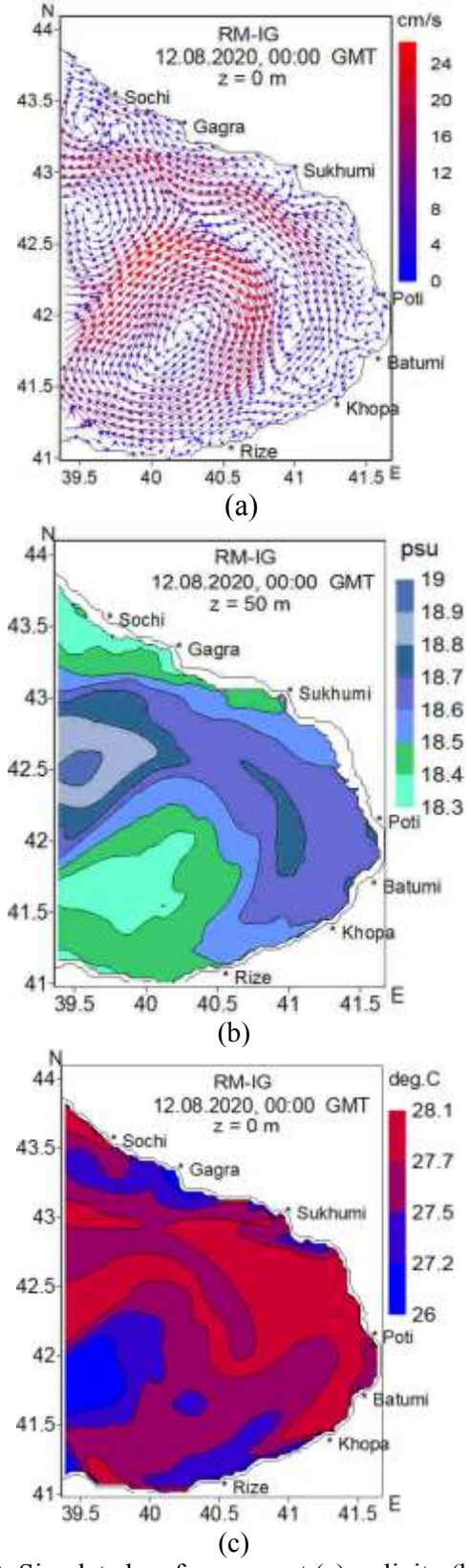

Fig. 2: Simulated surface current (a), salinity (b) at z = 50 m and SST (c) corresponding to 12 August 2020

Figure 2(a) clearly shows the Batumi anticyclonic eddy, which is the main element of the regional circulation for the mentioned day. The formation of small vortex structures is also observed. Comparison of the salinity field (Figure 2 (b)) with the velocity field (Figure 2(a)) shows a good correlation between these fields. The relatively low salinity in the central part of the anticyclone is due to the downward current, which transports low-salinity waters to the deep layers.

The SST correlates relatively weakly with the circulation structure, and the formation of the temperature field is largely determined by the exchange of heat between the sea and the atmosphere (Figure 2(c)).

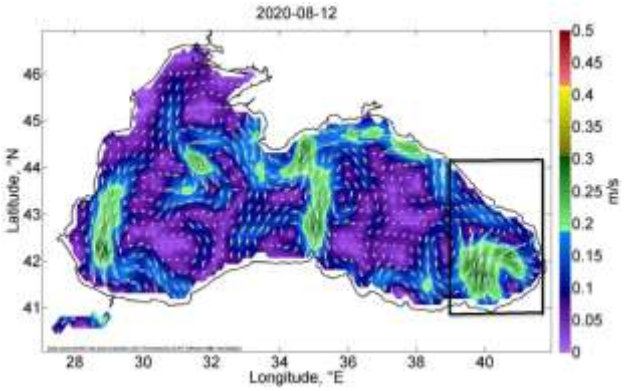

Fig. 3: Geostrophic surface current on 12 August, 2020, 00:00 GMT, which is created using satellite altimeter data. By rectangle, the forecasting area is marked

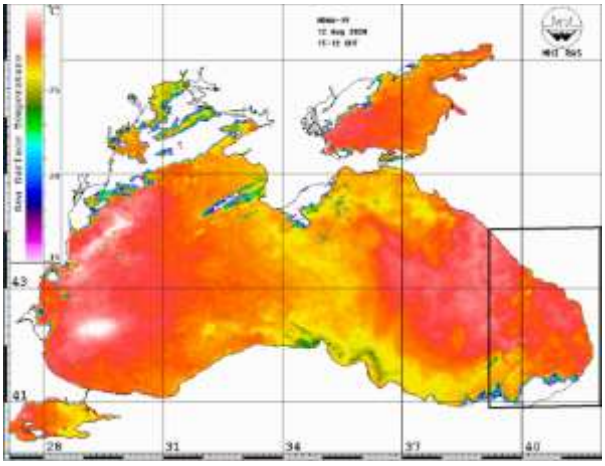

Fig. 4: Satellite SST corresponding to 15:12 GMT, 12 August, 2020. By rectangle, the forecasting area is marked

With the purpose of comparing forecasted fields with observational data, in Figure 3 the geostrophic current created using satellite altimeter data is presented for 12 August, 2020 and in Figure 4 – satellite SST derived from NOAA for 15:12 GMT, 12 August, 2020. Comparison of predicted surface circulation (Figure 2(a)) with the geostrophic current (Figure 3) shows that an anticyclonic eddy was actually observed for this day, as was obtained as a result of calculations.

Comparison of predicted (Figure 2(c)) and satellite SST (Figure 4) shows a good agreement with each other. According to both modeling results and satellite observations for 12 August 2020 water temperature on the most territory of the southeastern water area was 27-28^{0}C. Only on small territory in the southwestern part the temperature was about 26^{0}C.

With the purpose of a more quantitative comparison of the predicted and satellite SST fields, we calculated a root-mean-square error (RMSE) using the formula:

$$\mathrm{RMSE} = \sqrt{\frac{\sum_{k,l}(T^s_{k,l} - T^p_{k,l})^2}{N}}$$

where T^s is satellite SST and T^p – predicted SST, N –the number of grid nodes. It was found that for the considered day RMSE = 0,72^{0}c.

As can be seen from Figure 2(b) and Figure 2(c), the salinity and temperature fields in the upper layer are characterized by significant horizontal heterogeneity. Our calculations show that in the deep layers, below a depth of about 300 m, their horizontal gradients decrease significantly, which is in good agreement with the results of instrumental observations and numerical modeling, [1], [2]. The horizontal uniformity of thermohaline fields provides the barotropic nature of circulation in the deep layers of the Black Sea.

In Figure 5 velocity vector field is shown on horizons of 200, 500 and 1000 m for the same day.

It is clear from Figure 5 that the general anticyclonic nature of the mesoscale circulation is practically preserved in the 1000 m thick layer. Depending on the depth, the influence of the configuration of the sea basin increases and the circulation undergoes a certain transformation. On the horizon of 200 m, the Batumi eddy is well expressed, but its radius decreases. At the same time, the formation of small unstable eddies is observed. Due to the weakening of atmospheric forcing with depth, the current undergoes sharp quantitative changes: maximum speed on the sea surface 24 cm/s decreases to 12 cm/s on z = 200 m and to 4 cm/s on z= 1000 m. These speed values are

in good agreement with the profiling drifters ARGO data, [22].

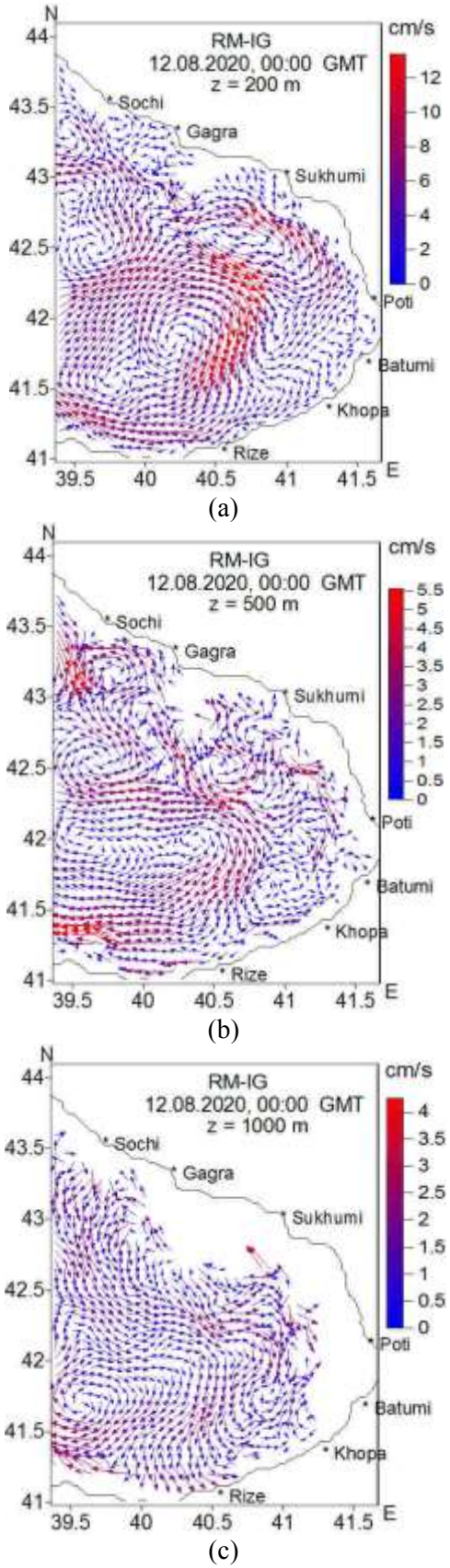

Fig. 5: Simulated current field on horizons of 200 m (a), 500 m (b) and 1000 m (c)

5 Conclusion

The paper presents a mathematical modeling method applied to simulate and forecast the hydrological regime of the southeastern part of the Black Sea. The effectiveness of the method, which is based on splitting the main differential operator into elementary operators, is demonstrated by modeling and forecasting of main hydrophysical fields – the current, temperature, and salinity - with 1 km spatial resolution for 12 August of 2020. Forecast outputs are compared with satellite data showing the reality of predicted fields.

In perspective, we plan to develop a high-resolution regional modeling system that will make it possible to simulate and forecast coastal dynamic processes with very high resolution in the Georgian nearshore zone with sizes of about 50-120 km, which is distinguished by high economic and recreational activity. With this purpose, a very high-resolution version of the RM-IG will be developed (with a spatial resolution 200 m). This advanced version, which will be nested in the RM-IG, will allow the simulation and forecast of nearshore processes with a higher accuracy.

Acknowledgment:
This work was supported by Shota Rustaveli National Science Foundation of Georgia (SRNSFG) [grant number FR-22-365].

References:

[1] Stanev E. V., Truhchev D. I., Roussenov V. M. *The Black Sea water circulation and numerical modeling of currents,* Kliment Ohridski University Press, Sofia, 1988, pp.222

[2] Kordzadze A. A. *Mathematical modeling of the current dynamics (theory, algorithms, Numerical experiments),* Moscow, OVM AN SSSR, 1989, 218 p (in Russian).

[3] Marchuk G. I., Sarkisyan A. S. *Mathematical modeling of Ocean Circulation.* Moscow, Nauka, 1988, 302 p (in Russian).

[4] Marchuk G. I., Kordzadze A. A., Skiba Yu. N. Calculation of the basic hydrological fields in the Black Sea, *Izvestiya USSR, Atmospheric and Oceanic Physics,* Vol.11, No. 4, 1975, pp. 229-237.

[5] Truhchev D. I., Demin Y. L. The Black Sea general circulation and climatic temperature and salinity fields. *Woods Hole Oceanographic Institution.* 1992, pp.1-13. https://doi.org/10.1575/1912/856.

[6] Marchuk G. I. *Methods of Numerical Mathematics.* Springer New York, 2011, pp.510.

[7] Zatsepin A. G., Baranov V. I., Kondrashov A. A., Korzh A. O., Kremenetsiy V. V., Ostrovskii A. G., Soloviev D. M. Submesoscale eddies at the Caucasus Black Sea shelf and the mechanisms of their generation. *Oceanology,*Vol. 51, No. 4, 2011, pp.554-567, https://doi.org/10.1134/S0001437011040205.

[8] Staneva J. V., Dietrich D. E., Stanev E. V**.,** Bouman M. J. Rim current and coastal eddy mechanisms in an eddy-resolving Black Sea general circulation model. *J. Mar. Sys.* 31, 2001, pp. 137-157, DOI: 10.1016/S0924-7963(01)00050-1.

[9] Kara A. B., Wallcraft A. J., Hurlburt H. E. New solar radiation penetration scheme for use in ocean mixed layer studies: An application to the Black Sea a fine resolution Hybrid coordinate ocean model (HYCOM). *J. Physic. Oceanography.* Vol.35, No. 1, 2005, pp.13-22. DOI: https://doi.org/10.1175/JPO2677.1.

[10] Stanev E. V. Understanding Black Sea dynamics: Overview of recent numerical modelling. *Oceanography,* Vol. 18, No. 2, 2005, pp. 56-75. https://doi.org/10.5670/oceanog.2005.42.

[11] Enriquez C. E., Shapiro G. I., Souza A. J., Zatsepin A. G. Hydrodynamic modelling of mesoscale eddies in the Black Sea. *Ocean Dynamics,* 55, 2005, pp.476-489, DOI: 10.1007/s10236-005-0031-4.

[12] Kordzadze A. A., Demetrashvili D. I., Surmava A. A. Numerical modelling of hydrophysical fields of the Black Sea under the conditions of alternation of atmospheric circulation processes. *Izvestiya RAS, Atmospheric and Oceanic Physics*. Vol. 44, No. 2, 2008, pp. 213-224, DOI: 10.1134/50001433808020096.

[13] Demyshev S. G., Dymova O. A. Analyzing intraannual variations in the energy characteristics of circulation in the Black Sea. *Izvestiya RAS, Atmospheric and Oceanic Physics*. Vol.52, No. 4, 2016, pp.386-393, https://doi.org/10.1134/s0001433816040046.

[14] Grigoriev A. V., Zatsepin A. G. Numerical modelling of water dynamics of Russian zone of the Black Sea within the framework of operational tasks. *J. Georgian Geophys. Soc.,* Vol. 16b, 2013, pp. 137-156.

[15] Zalesny V. B., Gusev A. V., Moshonkin S. N. Numerical model of the Hydrothermodynamics of the Black Sea and the Sea of Azov with variational initialization of temperature and salinity. *Izvestiya RAS, Atmospheric and Oceanic Physics*. Vol. 49, No. 6, 2013, pp. 699-716. https://doi.org/10.1134/S0001433813060133.

[16] Korotenko K. A. Predicting the behaviour of an oil spill in the Black Sea resulting from accidental offshore deepwater blowout. *J. Sustainable Energy Eng.* Vol. 6, No. 1, 2018, pp.48-83. DOI: 10.7569/JSEE.2018.629501.

[17] Korotenko K. A., Bowman M. J., Dietrich D. E., High-resolution numerical model for predicting the transport and dispersal of oil spilled in the Black Sea. *Terrestrial Atmospheric and Oceanic Sciences.* Vol. 21, No.1, 2010, pp. 123-136, DOI: 10.3319/TAO.2009.04.24.01(IWNOP).

[18] Korotaev G. K., Oguz T., Dorofeyev V. L., Demyshev S. G., Kubryakov A. I., Ratner Yu. B. Development of Black Sea nowcasting and forecasting system. *Ocean Science,* Vol.7, 2011, pp.629-649. DOI: 10.5194/os-7-629-2011.

[19] Kubryakov A. I., Korotaev G. K., Dorofeev V. L., Ratner Y. B., Palazov A., Valchev N., Malciu V., Matescu R., Oguz T., Black Sea coastal forecasting system. *Ocean Science,* Vol.8, 2012, pp. 183-196. https://doi.org/10.5194/os-8-183-2012.

[20] Kordzadze A. A., Demetrashvili D. I. Operational forecast of hydrophysical fields in the Georgian Black Sea coastal zone within the ECOOP. *Ocean Science*, Vol. 7, 2011, pp.793-803. DOI: 10.5194/os-7-793-2011.

[21] Andrews D. G. *An Introduction to atmospheric physics.* Cambridge University Press, 2010, pp.237.

[22] Markova N. V., Bagaev A. V. The Black Sea deep current velocities estimated from the data of Argo profiling floats. *Physical Ocoeanography,* 2016, 3, pp.23-35. DOI: 10.22449/1573-160X-2016-3-23-35.

Contribution of Individual Authors to the Creation of a Scientific Article (Ghostwriting Policy)

Demuri Demetrashvili developed software for a numerical solution algorithm in Fortran; conducted computational experiments, graphical interpretation and analysis of the obtained results and prepared a scientific article.

Sources of Funding for Research Presented in a Scientific Article or Scientific Article Itself

The work was supported by Shota Rustaveli National Science Foundation of Georgia (SRNSFG) [Grant number FR-22-365).

Conflict of Interest

The author has no conflicts of interest to declare.